

ICNMM2008-62070

LOW-REYNOLDS-NUMBER INSTABILITY OF THE LAMINAR FLOW BETWEEN WAVY WALLS

Tomasz A. Kowalewski, IPPT PAN, Polish Academy of Sciences, Warsaw, Poland, tkowale@ippt.gov.pl

Jacek Szumbariski, Warsaw University of Technology, Warsaw, Poland, jasz@meil.pw.edu.pl

Slawomir Blonski, IPPT PAN, Polish Academy of Sciences, Warsaw, Poland, sblonski@ippt.gov.pl

ABSTRACT

Instability of a viscous incompressible flow in a channel with wavy walls is investigated theoretically, numerically and experimentally. Linear stability analysis shows that appropriately chosen wall waviness leads to flow destabilization at surprisingly low Reynolds numbers. The unstable mode of disturbances forms a vortex array, which travels downstream. The remarkable feature is that the most destabilizing waviness does not introduce any additional flow resistance. The outcome of the stability analysis are consistent with the result of direct numerical simulation obtained using CFD finite volume package FLUENT (Ansys Inc.). Preliminary experimental data gained for a channel with appropriately corrugated wall seem to confirm these predictions.

NOMENCLATURE

Symbol	Description	Unit
$2H$	Channel height	m
p	Pressure	Pa
Re	Reynolds number	-
S	Wall corrugation amplitude	-
Q_V	Volumetric flow rate	m ³ /s
u, v, w	Velocity components	m/s
W_{max}	Maximum velocity	m/s
V'	Fluctuation of velocity	m/s
α	Corrugation wave number	-
μ	Dynamic viscosity	Pas

INTRODUCTION

Enhancement of mixing in the laminar regime is of fundamental importance in numerous applications in microfluidics, biotechnology, medicine and heat transfer [1]. Significant improvement of mass and/or heat transfer can be achieved only if sufficiently complex and time-dependent vortex structures are present. Such structures can be triggered by various geometric modifications (e.g., the wall waviness or surface-mounted obstacles), external forcing (e.g. oscillations

of a driving pressure gradient) or the combination of both [2,3]. Unfortunately, in most cases the mixing improvement is accompanied by large increase of hydraulic resistance.

The current work describes the mixing-enhancement method based on the idea of forced chaotic convection in the channel with appropriately shaped and transversely oriented wall waviness. The method is based on results of linear stability analysis applied to a simple unidirectional flow in a wavy channel. It was demonstrated in [4,5] that the laminar flow in the channel with properly tuned, transversely-oriented wall waviness can spontaneously lose stability at the Reynolds numbers as low as 60. Following this idea, the three-dimensional numerical simulations of viscous flow through wavy channel are performed both for the infinite flow domain (periodic boundary conditions) and for the channel bounded by the side walls. The positive outcome of the numerical computations gave us confidence to the theoretical predictions, necessary to design microchannel mixer. Finally, the flow structures observed for laminar flow of water in a 33.6 mm wide wavy microchannel are investigated to identify predicted instabilities.

STABILITY ANALYSIS

Consider the reference case: the laminar incompressible flow in the region between two parallel planes $Y = -H$ and $Y = H$. Let $G_p < 0$ denotes the constant pressure gradient which drives the fluid in the positive direction of the Z axis. The velocity field can be expressed as

$$\mathbf{V}_0 = [0, 0, W_0(Y)] = \left[0, 0, W_{max} \left(1 - \frac{Y^2}{H^2} \right) \right] \quad (1)$$

In (1), μ denotes the dynamic viscosity and W_{max} is the maximal velocity given by the formula

$$W_{\max} = -\frac{G_p H^2}{2\mu}$$

Define the length scale H , the velocity scale W_{\max} and the pressure scale ρW_{\max}^2 , where ρ denotes the density of the fluid. Then, the velocity field (1) is transformed to the standard Poiseuille flow

$$w_0(y) = 1 - y^2 \quad (2)$$

where the dimensionless coordinate $y=Y/H$ belongs to the interval $[-1,1]$. The nondimensional pressure gradient can be now expressed by the Reynolds number $\text{Re} = W_{\max} H \rho / \mu$ as

$$g_p = G_p \frac{H}{\rho W_{\max}^2} = -\frac{2}{\text{Re}}$$

Consider now the laminar flow in the wavy channel (Figure 1). The shape of the channel walls is described by the x -periodic functions (period is equal $\lambda_x = 2\pi/\alpha$)

$$y_{-1,1}(x) = -1 + \sum_{(m)} A_{-1,1}^m \exp(im\alpha x) + C.C. \quad (3)$$

where ‘‘C.C.’’ stands for the complex conjugate terms, and subscripts ‘‘-1’’ and ‘‘1’’ refer to the lower and upper channel wall, respectively. The flow in the wavy channel is driven by the same pressure gradient as the reference Poiseuille flow and the corresponding velocity field can be expressed as

$$\mathbf{v}_B = [0, 0, W(x, y)] \quad (4)$$

The function W is x -periodic and it can be determined as the solution to the following boundary-value problem

$$\begin{aligned} \Delta W &= -\text{Re } g_p \equiv 2 \\ W(x, y_{-1}(x)) &= 0, \quad W(x, y_1(x)) = 0 \end{aligned} \quad (5)$$

where $\Omega = \{(x, y) : x \in (0, \lambda_x), y_{-1}(x) < y < y_1(x)\}$ and $\Delta = \partial_{xx} + \partial_{yy}$.

The problem (5) can be solved using the following semi-analytical approach. We introduce the extended domain

$$\Omega_{\text{ext}} = \{(x, y) : x \in \mathbf{R}, y \in [y_{\min}, y_{\max}]\}$$

where $y_{\min} = \min_{x \in [0, \lambda_x]} y_{-1}(x)$ and $y_{\max} = \max_{x \in [0, \lambda_x]} y_1(x)$.

Clearly, the inclusion $\Omega \subset \Omega_{\text{ext}}$ holds. Next, we define

$$W(x, y) = w_0(y) + W'(x, y) = 1 - y^2 + W'(x, y).$$

where $(x, y) \in \Omega_{\text{ext}}$. The component $W'(x, y)$ describes the modification of the reference flow due to the wall corrugation. The Poisson equation (5) is satisfied providing that the function

$W'(x, y)$ is harmonic in Ω_{ext} , i.e., it fulfills the Laplace equation $\Delta W' = 0$.

The real harmonic function W' can be expressed in the form of the Fourier series

$$\begin{aligned} W'(x, y) &= C_0 + D_0 y + \\ &+ \sum_{n \neq 0} [C_n \cosh(n\alpha y) + D_n \sinh(n\alpha y)] e^{in\alpha x} \end{aligned} \quad (6)$$

where C_0 and D_0 are real and $C_{-n} = C_n^*$, $D_{-n} = -D_n^*$ for all $n \neq 0$. The coefficients $\{C_n\}$ and $\{D_n\}$ should be such that the boundary conditions in (5) are satisfied. To this end, the Fourier coefficients of the velocity distributions along the wavy walls are calculated and set to zero. In the practical implementation, only a finite number of the leading Fourier modes can be eliminated. It has been shown recently in by Szumbariski [4] that the least squares formulation of such elimination procedure is particularly efficient and spectrally convergent. In this approach, the number of the (approximately) eliminated Fourier harmonics is larger than the number of the unknown coefficients in the truncated series (6).

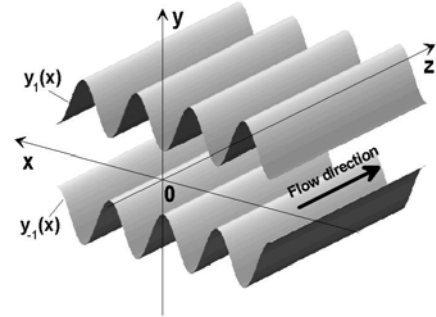


Figure 1: Channel with transversely wavy walls.

The further analysis focuses on the special case of the wall waviness, which is – as we will see later – the best configuration to achieve the low Reynolds number destabilization. We assume that the walls are sinusoidal with the amplitude S and the channel is symmetric with respect to the center plane $y = 0$, i.e.

$$y_{-1}(x) = -1 - S \cos \alpha x, \quad y_1(x) = 1 + S \cos \alpha x \quad (7)$$

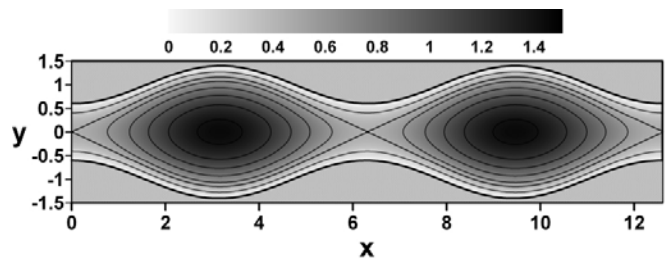


Figure 2: The contour map of the velocity of the basic flow. The wave number $\alpha = 1$, the amplitude $S = 0.4$.

The effect of the wall waviness depends strongly on the wave number α . If α is large (short wave) then the flow modifications are confined to the narrow regions adjacent to the walls, while the shape of the velocity profile in the “core” part of the flow remains nearly parabolic. If α gets smaller (longer wave) the flow modifications expand gradually towards the symmetry plane $y = 0$ and eventually take form of the large-amplitude spanwise modulation. The emerged “streaky” flow is prone to destabilization even at rather low Reynolds number. The contour map of the corresponding velocity field, computed for $S = 0.4$ and $\alpha = 1$ is shown in the Figure 2. Another interesting issue is how the transversal wall waviness affects the flow resistance. It turns out that long-wave waviness (α around 1 or less) can provide a noticeable drag reduction [4].

In order to determine the stability properties of this flow, small time-dependent disturbances of the velocity $\mathbf{v}' = [u', v', w'](t, x, y, z)$ and of the pressure $p' = p'(t, x, y, z)$ are introduced. The velocity and pressure of the basic flow is given as $\mathbf{v}_B = W(x, y)\mathbf{e}_z$ and $p_B = -(2/\text{Re})z$. The velocity and pressure of the disturbed flow can be written as

$$\mathbf{v} = \mathbf{v}_B + \mathbf{v}' \quad , \quad p = p_B + p' . \quad (8)$$

By inserting (8) into the Navier-Stokes and continuity equations and skipping the nonlinear terms, one arrives at the following linear system

$$\partial_t u' + W \partial_z u' = -\partial_x p' + \frac{1}{\text{Re}} \Delta u' . \quad (9a)$$

$$\partial_t v' + W \partial_z v' = -\partial_y p' + \frac{1}{\text{Re}} \Delta v' \quad (9b)$$

$$\begin{aligned} \partial_t w' + W \partial_z w' + u' \partial_x W + v' \partial_y W = \\ = -\partial_z p' + \frac{1}{\text{Re}} \Delta w' \end{aligned} \quad (9c)$$

$$\partial_x u' + \partial_y v' + \partial_z w' = 0 \quad (9d)$$

We will focus on the special solutions of the equations (9) known as the normal modes [6]. These solutions are crucial for the determination of the asymptotic behavior of small disturbances in the flow. Since the coefficients of the above equations are x -periodic, the admissible form of the normal modes is

$$\begin{aligned} [u, v, w](t, x, y, z) = \\ = e^{i(\delta x + \beta z - \sigma t)} \sum_{m=-\infty}^{\infty} [g_u^m, g_v^m, g_w^m](y) e^{im\alpha x} + C.C. \\ p'(t, x, y, z) = \\ = e^{i(\delta x + \beta z - \sigma t)} \sum_{m=-\infty}^{\infty} q^m(y) e^{im\alpha x} + C.C. \end{aligned} \quad (10)$$

In the above, the symbol β denotes the streamwise wave number, δ is the Floquet parameter and the number $\sigma = \sigma_R + i\sigma_I$ is the complex frequency of the normal mode. Thus, the formulae (10) describe the disturbance, which are

periodic in z direction (the period $\lambda_z = 2\pi/\beta$) and - dependently on the ratio δ/α - periodic or quasi-periodic in x direction.

The time variation of the normal mode is determined by its complex frequency σ . If σ_I is negative then the mode is attenuated or stable. If σ_I is positive then the mode is amplified or unstable. In $\sigma_I = 0$ then the mode is neutrally stable or critical. All normal modes are stable if the Reynolds number is sufficiently small. As the Reynolds number increases, some normal mode(s) may become unstable. Existence of such mode(s) is the sufficient conditions for the flow destabilization by disturbances of arbitrary small magnitude. The upper limit of the Reynolds number for which all normal modes are stable (or neutral) is called the critical Reynolds number Re_L . For the reference Poiseuille flow, Re_L is equal approximately 5772 [6].

The real part of the complex frequency determines the kinematic character of the disturbance field. If $\sigma_R \neq 0$ then the disturbances have the form of the traveling wave (the speed of this wave in streamwise direction is equal σ_R/β). Such disturbances are also called the oscillatory ones because at any fixed point in space one observes time-periodic modulation of the disturbance amplitude (superimposed on the exponential decay or growth). If $\sigma_R = 0$ then time variation of the amplitude of disturbances at any space location is monotonic (non-oscillatory); such disturbances are sometimes called stationary.

Substitution of the expressions (10) into the equations (9) leads to a countable set of the ordinary differential equations for the amplitude functions g_u^m , g_v^m , g_w^m and q^m , ($m = \dots, -2, -1, 0, 1, 2, \dots$). The mathematical description of the disturbance dynamics can be simplified in the case of parallel flows [6] by eliminating pressure and introducing the y -component of the vorticity with the formula

$$\eta = \sum_{m=-\infty}^{\infty} \theta^m(y) e^{i(t_m x + \beta z - \sigma t)} + C.C. \quad (11)$$

where

$$\theta^m = i(\beta g_u^m - t_m g_w^m) \quad (12)$$

and $t_m = \delta + m\alpha$, $m = 0, \pm 1, \pm 2, \dots$. Using the relations (12) together with the formulae implied by the continuity equation

$$it_m g_u^m + \partial_y g_v^m + i\beta g_w^m = 0 \quad (13)$$

one can express the amplitude functions of the velocity components u and w by the velocity component v and the vorticity components η , namely

$$\begin{aligned} g_u^m &= i(t_m \partial_y g_v^m - \beta \theta^m) / k_m^2 \\ g_w^m &= i(\beta \partial_y g_v^m + t_m \theta^m) / k_m^2 \end{aligned} \quad (14)$$

In the above, we have introduced the real numbers $k_m^2 = t_m^2 + \beta^2$, which must be different from zero for all integer indices m . The latter condition is always satisfied if the streamwise wave number $\beta \neq 0$, which is assumed in this study.

In order to obtain a numerically tractable problem, the Fourier representation of the disturbance field is truncated to a finite number of modes and all amplitude functions g_v^n and θ^n are approximated by finite Chebyshev expansions [5].

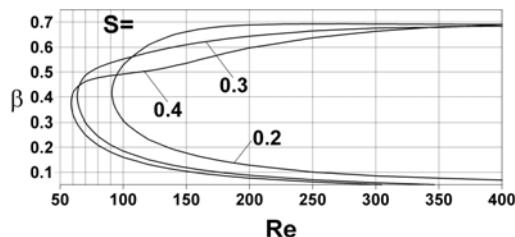


Figure 3: The lines of neutral stability of the fundamental transverse Squire's mode, computed for the flow in the symmetric channel with sinusoidal walls (see Figure 2). Results for three different amplitudes S are shown, the wave number $\alpha = 1$.

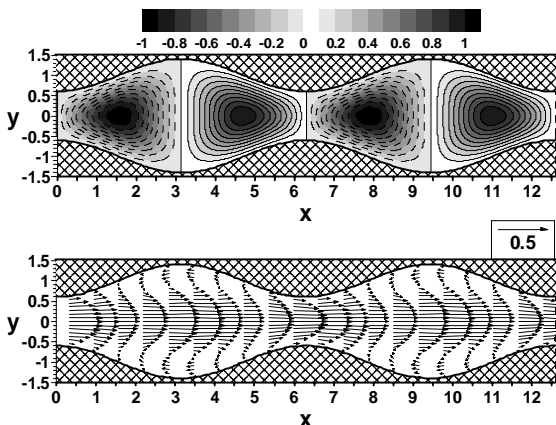


Figure 4: The normalized disturbance velocity field calculated for the Reynolds number $Re = 60$; the amplitude is $S = 0.4$, and the geometric wave number is $\alpha = 1$. The contour map shows magnitude of the streamwise velocity component (dashed lines correspond to negative values).

Identification of an unstable mode(s) can be done effectively by parametric continuation of selected eigensolutions of the Orr-Sommerfeld and Squire equations corresponding to the reference Poiseuille flow [6]. In the case of the sinusoidal shape (7), it is natural to choose the amplitude S as the continuation parameter, while the appropriate numerical tool is the method of inverse iterations. The key problem is to identify an eigenmode of the Poiseuille flow, which is most prone to destabilization by the particular geometrical modification of the flow domain. It is well established fact [7] that short-wave transversal wall corrugation destabilizes the fundamental two-dimensional Orr-Sommerfeld mode and the critical Reynolds number can be lower down to about 2500. In view of the possible application in laminar mixing, this number is still much too high to be useful. There exists, however, a different normal mode - the fundamental transversal Squire's mode - which is particularly sensitive to

destabilization by a long-wave transversely-oriented wall corrugation. In the reference flow, this mode has the form of the wave traveling downstream with the velocity slightly smaller than the maximal velocity in the mean flow, and attenuated asymptotically for all Reynolds numbers. It turns out that the transverse corrugation with the wave number $\alpha \approx 1$ can very effectively destabilize this mode and the critical Reynolds number can be easily lowered under 100, especially when both walls are corrugated in the opposite phase (symmetric channel). This effect is illustrated in the Figure 3 where the curves of neutral stability, (i.e. the lines $\sigma_l = 0$) in the Re - β plane are shown. It can be seen that the critical Reynolds number Re_L for the amplitude $S = 0.4$ is approximately equal 58, i.e., it is smaller by two orders of magnitude that Re_L for the reference Poiseuille flow. It should be emphasized that such radical reduction of Re_L is achieved in the range of α 's where no additional flow resistance is generated.

It has been demonstrated [5] that the effect of destabilization depends very weakly on geometrical details of the wall waviness. In other words: what is crucial for the flow destabilization is the spectral content of the wall shape rather than the overall amplitude of the corrugation. Roughly speaking, any shape of waviness will do the job if only its spanwise period is 3-4 time larger than the average channel's height and the amplitude of the fundamental Fourier mode in the series (3) is sufficiently high. Recently it has been also established for the sinusoidal waviness that the lowest critical Reynolds number $Re_L \approx 57.4$ is achieved for the amplitude $S = 0.392$ and the wave number $\alpha = 1.039$.

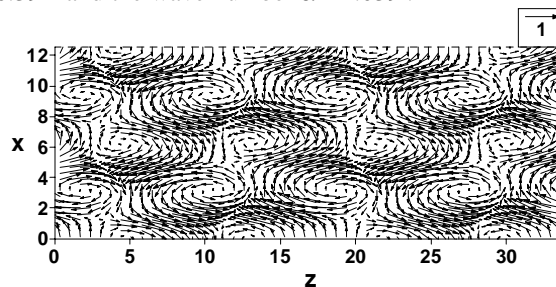


Figure 5: The structure of the (normalized) velocity field of the unstable Squire's mode in the channel's symmetry plane $y = 0$. All parameters like in the Figure 4.

The kinematic structure of the unstable mode is an important issue, particularly in the context of laminar mixing. The streamwise structure of the normalized velocity disturbances, computed for $S = 0.4$, $\alpha = 1$ and $Re = 60$ is presented in Figure 4. The upper plot shows the contour map of the streamwise velocity component w in the plane $z = 0$, while the bottom one presents the velocity vectors projected on the same plane. Figure 5 shows the same field in the channel's centerplane $y = 0$. The presence of space-periodic structure of counter-rotating vortices is evident. Since $\sigma_R \neq 0$, this mode describes oscillatory disturbances, i.e. having the form of the traveling wave. The speed of the downstream propagation is equal 0.85, which is slightly less than the average velocity of the fluid in the channel centerplane.

NUMERICAL ANALYSIS

Predictions of the stability analysis are verified using numerical simulation of the viscous, incompressible, unsteady

fluid flow through the wavy channel. Finite-volume package Fluent 6.3 (Ansys Inc.) is used to generate the computational grid and to perform stability analysis using unmodified three-dimensional set of Navier-Stokes equations (DNS). The DNS model allows to obtain accurate, unsteady solution of unmodified Navier-Stokes equations by resolving the whole range of spatial and temporal scales of the turbulence. In our case the main aim of the simulation is to identify presence of transversal instability modes and the critical Reynolds number for their amplification. The numerical domain used in the simulations had to cover full 3D geometry of the physical channel and all spatial scales of the turbulence should be resolved in the computational mesh. Hence, very fine mesh and small time steps are used. The direct numerical simulation performed with the classical finite volume code is time consuming and vulnerable. Nevertheless, it appeared in our previous study [8] that it permits to obtain reasonable DNS solution reproducing typical for the turbulent flow characteristics.

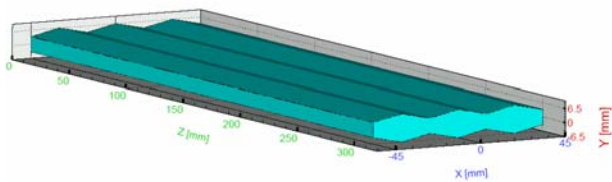


Figure 6: Computational domain used for simulating flow in the infinite channel with two corrugated walls. Periodic boundary conditions are assumed for two side walls, the inlet and the outlet.

Analytical model described above assumes infinite domain. In the first numerical configuration the analytical model assuming flow between two infinite walls is imitated simulating periodic boundary conditions in spanwise and streamwise direction. The computational domain is limited to three periods of waviness in spanwise direction and non-slip boundary condition is assumed for upper and lower wall only (Fig. 6). The selected waviness of the wall geometry is close to the optimal predicted by the linear stability analysis: wavelength $\alpha = 1$ and the waviness amplitude $S = 0.3$.

For any physical channel side walls, inlet and outlet are unavoidable and they presence may substantially modify predictions of the theoretical model. In the second computational configuration impact of the confine channel geometry on the flow stability is analyzed. The computational domain describes channel with five periods of waviness in the spanwise direction closed by two side walls with non-slip kinematic boundary conditions. Still the channel is infinite in the streamwise direction (periodic boundary conditions for the inlet and the outlet).

In both computational models structural hexahedron mesh with boundary layer was generated. The boundary layer mesh had five nodes and linear growth factor of 1.2. Several mesh resolution tests were performed to identify the optimal discretization, being compromise of the computational time and the numerical accuracy. The optimal mesh resolution was selected using Grid Convergence Index [9]. It was mesh of about 405000 elements for the infinite channel and 675000 elements for the confined channel. The unsteady, double precision, segregated solver with SIMPLE pressure correction

was used. The time stepping was performed using implicit, second order Adams-Bashforth upwind scheme keeping all residuals reduced to 10^{-6} . The optimal time step of the simulation was estimated by performing several computational tests. It was found to be equal 10^{-2} s. Using this time step it took us about 3 weeks of CPU time to obtain solution of 100s flow time on Pentium D (3GHz) node of the department Mosix cluster [10].

The main parameter of the analyzed flow is Reynolds number. The fully developed turbulent flow was obtained for $Re = 3000$ applying properties of water (viscosity and density) in the numerical model. To find out stability limits the computations were repeated decreasing Reynolds number down to one. The flow Reynolds number was decreased by appropriate increase of the fluid viscosity, whereas the mass flow rate was set constant and equal $6 \cdot 10^{-3}$ kg/s. Such procedure allowed us to initiate new numerical solution with a disturbed flow structure obtained from the previous calculations performed at higher Reynolds number, reducing overall computational time.

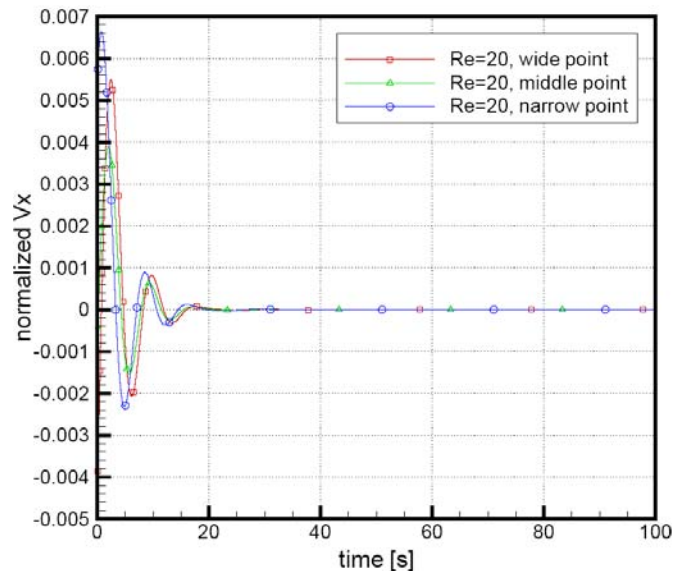


Figure 7: Damping of the initial disturbances of spanwise velocity component extracted from the numerical simulations of flow in the infinite channel at Reynolds number $Re = 20$.

The flow stability analysis was performed for 13 Reynolds numbers: 1, 10, 20, 30, 40, 50, 60, 70, 100, 200, 500, 1000 and 3000. Damping or amplification of flow disturbances initially present from the previous solution was analyzed by monitoring spanwise velocity fluctuations at three points selected at the channel symmetry plane. They were chosen in the symmetry plane $y=0$ at spanwise locations corresponding to the maximum and minimum channel high, and between both.

Figure 7 illustrates fast damping of the initially perturbed velocity field observed for $Re = 20$. We may find that after less than 20s all fluctuations vanish and the flow becomes stationary. The opposite behavior can be found for higher Reynolds number, namely $Re = 100$ (Fig. 8). Initial flow disturbances are obviously amplified and after about 200 s fully developed unsteady flow is observed. The flow velocity field extracted from the numerical solution for the channel

central cross-section well reproduces predicted by the linear stability analysis space periodic counter-rotating vortices (Fig. 9) traveling in the streamwise direction. It seems evident that the introduced wall waviness generates spanwise instabilities propagating along the channel and disturbing the flow structure. The new unstable flow pattern which emerges from the unstable mode have complex three-dimensional structure promoting mixing properties of the channel flow. It is interesting to note that presence of the side walls (confined channel) does not significantly change this picture. Numerical simulations performed for the confined channel with five waviness periods only show that except regions in vicinity of the side walls, the flow structure with the characteristic transversal vortices appears to be present for Reynolds number above 100.

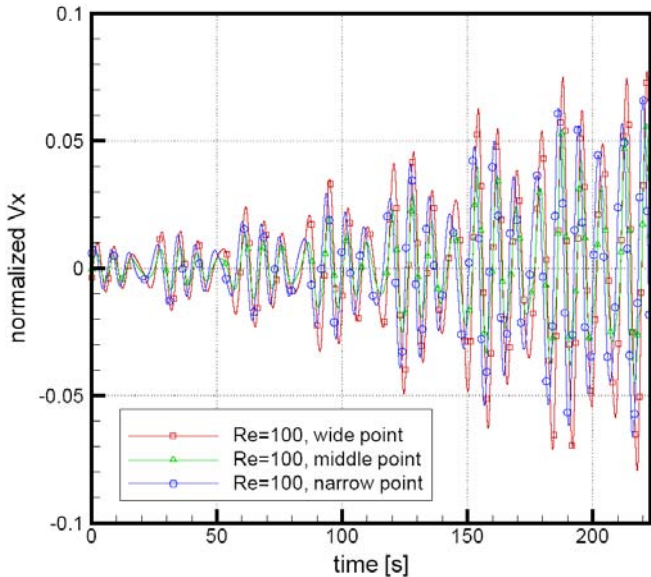


Figure 8: Amplification of the initial disturbances of spanwise velocity component extracted for three points from the numerical simulations for flow in the infinite channel at Reynolds number $Re = 100$.

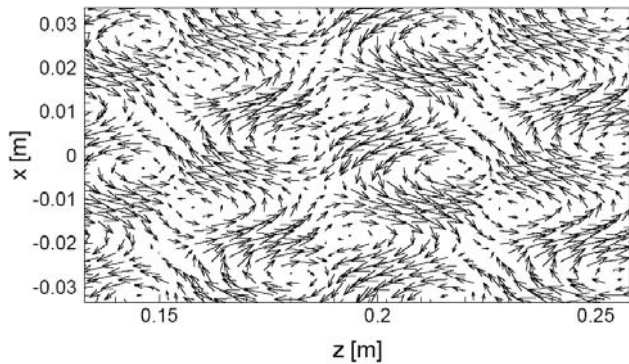


Figure 9: Disturbed flow pattern obtained from the numerical simulations for the symmetry plane ($y = 0$), flow Reynolds number $Re = 100$.

The effect of flow Reynolds number on amplification ratio of the unstable mode predicted by the linear stability analysis is given in Figure 10. We may find that unstable modes (positive amplification factor) appear shortly above Reynolds

number 50. This theoretical prediction is compared with the amplification ratio of the velocity fluctuations obtained from the numerical simulations. This ratio was obtained by evaluating slope of the velocity oscillation amplitude monitored at selected flow points. It can be seen in Figure 10 that numerical simulations confirm value of the predicted critical Reynolds number to be slightly above 100. The fully saturated instability is obtained at Reynolds number $Re = 250$, one order of magnitude below the critical Reynolds number for the channel flow between two plane walls.

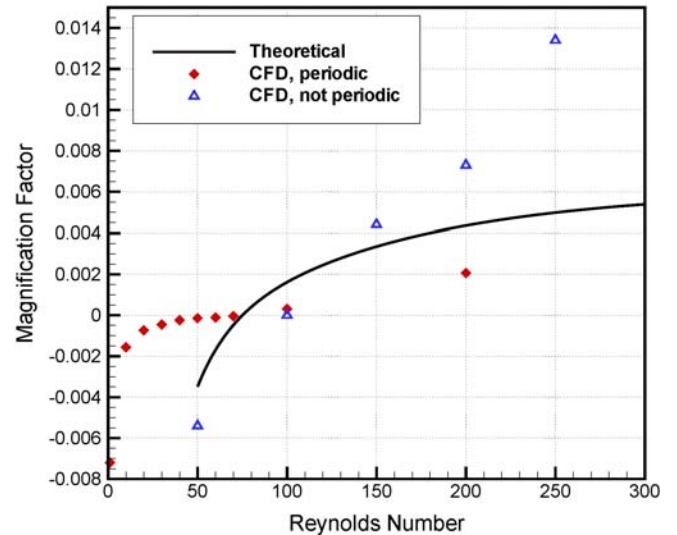


Figure 10: Amplification ratio of unstable transversal modes (in arbitrary units): predicted by the linear stability analysis (solid line); numerical simulation between infinite corrugated walls (diamonds); numerical simulations for the flow in the corrugated channel confined by side walls (triangles). Positive values indicate amplification of the disturbance amplitude.

EXPERIMENTAL

A simple model of the wavy channel formed between two plates has been machined in polycarbonate using micro-machining technique. The average channel height is $793 \mu\text{m}$, its width is 33.6 mm , and the length 75 mm . Surface of the bottom wall is modulated by 20 rows (comp. Fig. 11). They create spanwise periodic structure with channel depth varying from 0.4 mm to 1 mm . The upper wall of the channel is flat to permit optical measurements.

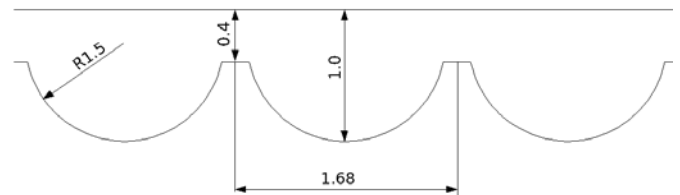


Figure 11: Geometry of the bottom wall corrugation in the experimental channel. The top wall is flat for better optical access.

The 4.5 mm tubes are connected to the divergent channel entry and convergent outlet. The flow is driven by the micro pump (Cole-Palmer Inst.) permitting flow rate variation from

$Q_V = 0.02 \text{ cm}^3/\text{s}$ to $70 \text{ cm}^3/\text{s}$. An average flow velocity in the channel can be varied from about 0.76 mm/s to 2.6 m/s , which corresponds to Reynolds number based on the average channel height $Re=0.6$ and $Re=2100$, respectively. The channel length is probably too short to allow for fully developed flow instabilities to occur spontaneously. However, it is assumed that initial spanwise flow disturbances generated by the strongly divergent flow inlet may become amplified by the wall waviness, if the theoretical prediction is correct.

The flow of deionised water is examined through the top wall of the channel using epi-fluorescence microscope (Nikon Eclipse 50i). The flow is seeded with fluorescent polystyrene spheres, $2\mu\text{m}$ in diameter (Duke Scientific Inc.). Two different light sources are used to excite fluorescence of the tracer particles: built-in mercury lamp for particle tracking and Nd:YAG 30mJ (532nm) double pulsed laser for the flow velocity measurements (micro-PIV) [8]. For the flow imaging two high-resolution (1280×1024 pixels) 12bit cameras are used: *PCO SensiCam* camera for the PIV measurements, and high speed camera *PCO1200hs* for the flow visualisation and particle tracking.

The flow is observed using 10x (NA 0.3 / WD 17.30 mm) microscope lens approximately 60mm from the channel inlet at its symmetry axis. The area covered by the camera is $854 \mu\text{m} \times 683 \mu\text{m}$.

For the flow visualisation long time exposure (120 ms) of single fluorescent traces is done. These experiments allow for fast identification of the critical Reynolds number. At low flow rates the particle tracks exhibit straight lines. Increasing flow rate the wavy character of particle tracks reveals emerging transversal flow disturbances. Our preliminary experimental study shows that transversal velocity fluctuations can be visualized by particle tracking at least for flow Reynolds number $Re = 100$. Figure 12 illustrates typical disturbances of the particle track observed for the fluorescent tracer for the flow at Reynolds number $Re=120$. The wavy motion of the tracer implies presence of the transversal velocity component.

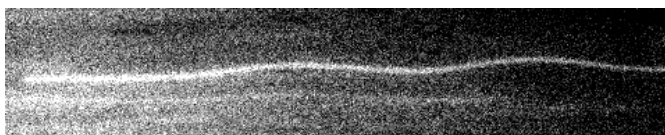


Figure 12: Trace of the fluorescent particle recorded in the corrugated channel (Fig. 11). The image width corresponds to 0.3mm , illumination time is 0.12s , flow Reynolds number $Re=120$.

Micro-PIV measurements provide quantitative data about flow field disturbances. Two sets of measurements are performed shifting the observation area across the channel from the wall protrusion to its dimple. At each position the flow is interrogated at five different vertical positions. As a result, ten sets of velocity fields are obtained from the micro-PIV measurements - each of them at different location. At each location 200 pairs of images are acquired for further evaluation of the vector velocity fields. The average flow velocity is subtracted from the PIV results to obtain the flow disturbances only.

The typical velocity field structure obtained by means of micro-PIV is given in Fig. 13. The mean flow is subtracted to reveal transversal velocity components. Due to small

interrogated flow area ($0.85 \text{ mm} \times 0.68 \text{ mm}$) only flow in the vicinity of a single corrugation can be shown. Nevertheless, one may find that local spanwise flow disturbances are present, indicating emerging flow instabilities. The transversal flow disturbances are generated across the whole channel width, interacting in a complex way with all 20 corrugations. Proper understanding of the full structure of the analysed flow needs recombination of several sets of single flow fields obtained at different locations across the channel, and at its different depths. These flow structures measured by means of micro-PIV are still under evaluation. For better understanding the experimental data it seems necessary to repeat numerical simulations of flow in a geometry exactly reproducing our physical channel.

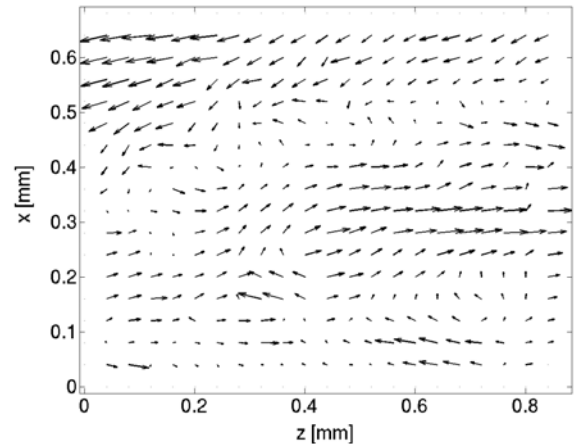


Figure 13: Disturbed velocity field measured in the corrugated channel 0.2 mm below the upper wall. The image width corresponds to 0.85 mm , flow Reynolds number $Re = 150$.

CONCLUSIONS

Numerical simulations of viscous incompressible flow in a channel with transversely corrugated channel walls confirms predicted by the linear stability analysis exponentially growing flow instability at the Reynolds numbers as low as 60. Preliminary experimental study in a small channel with a single corrugated wall seems to support this prediction. However, more detailed study is necessary to compare the predicted complex and time-dependent structures of the disturbed flow with the experimental measurements. Parametric study is necessary to elucidate effects of the finite channel dimensions, the inlet and outlet initial disturbances, and of the side walls position on the disturbance amplification. These physical constraints have to be included as additional parameters for future evaluation of the optimal amplitude and wavelength of the wall waviness.

ACKNOWLEDGMENTS

This investigation was supported by the Polish Ministry of Science and Education under project *Enhancement of the mixing process in micro-flows*, grant No.: N501008733.

REFERENCES

- [1] King K.R., Wang S., Irimia D., Jayaramn A., Toner M., Yarmush M., A high throughput microfluidic realtime gene expression living cell array, *Lab on Chip*, vol. 7, pp. 77-85, 2007.

- [2] Nguyen N. T., Wu, Z., Micro-mixers – a review, *J. Micromech. Microeng.* 15, pp. 1-6, 2005
- [3] S. Hardt S., Pennemann H., Schönfeld F., Theoretical and experimental characterization of a low-Reynolds number split-and-recombine mixer, *Microfluid. Nanofluid.* 2, pp. 237-248, 2006.
- [4] Szumbariski J, Instability of viscous incompressible flow in a channel with transversely corrugated walls, *J. of Theor. and Appl. Mechanics* 45, pp.659-684 , 2007
- [5] Szumbariski J., *Instability of a viscous liquid flow in the wavy channel.* Habilitation dissertation (in Polish), Scientific Works of Warsaw University of Technology, vol. 218, 172 pages, Warsaw 2007.
- [6] Schmid P.J., Henningson D.S.: Stability and Transition in Shear Flows. Applied Mathematical Sciences 142, Springer New York, 2001.
- [7] Ehrenstein U., 1996: On the linear stability of channel flow over riblets. *Physics of Fluids* 8, pp. 3194-3196, 2007.
- [8] Kowalewski T.A., Błoński S. Korczyk P., 2006, Turbulent Flow in a Microchannel, *Proc. of ASME ICNMM2006*, CD-ROM paper 96090, Limerick, Ireland
- [9] Roache P.J., “Verification and validation in Computational Science and Engineering”, Hermosa Publishers, Albuquerque, NM, 1998
- [10] Department Mosix cluster: <http://fluid.ippt.gov.pl/mosix/>